International Journal of Applied Power Engineering (IJAPE)
Vol. 14, No. 4, December 2025, pp. 1011~1022
ISSN: 2252-8792, DOI: 10.11591/ijape.v14.i4.pp1011-1022

Improve the thermal performance of the combined water-paraffin hot storage tank in the absorption cooling cycle

Maki Haj Zaidan, Thamir Khalil Ibrahim, Hussam S. Dheyab
Department of Mechanical Engineering, College of Engineering, Tikrit University, Tikrit, Iraq

Article Info

Article history:

Received Jun 15, 2025
Revised Aug 23, 2025
Accepted Oct 16, 2025

Keywords:

Absorption cooling system
Concentric parabolic collectors
Paraffin PCM
Phase change material
Storage tank

ABSTRACT

This research investigates the thermal performance of storage materials in a hot tank designed to extend the operation time of a 1.5-ton water ammonia absorption cooling system. Thermal energy is supplied by concentric parabolic solar collectors, which heat the absorption cycle generator during periods of sufficient solar radiation. When the water temperature exceeds the system's operating threshold, the additional heat accumulates in the hot tank. It is later used to drive the generator during periods of low solar availability, such as in the afternoon or after sunset. The system is designed to provide air conditioning for a room; its load was calculated hourly. The suitable size of the storage tank and the corresponding collector area were determined based on simulations of the absorption system to achieve an optimal coefficient of performance (COP). The collector area was increased after the addition of paraffin phase change material (PCM) to enhance system performance, and a temperature control strategy was implemented to prevent the water in the hot storage tank from reaching the boiling point. This was achieved by incorporating a specific percentage of paraffin, a PCM, with a melting point of 85 °C. The size of the hot storage tank containing both water and a specified proportion of paraffin, in addition to the solar collector area, was optimized to maximize the tank temperature. These parameters were entered into the energy balance model as input data to ensure the effective operation of the absorption system under optimal conditions. A comprehensive system simulation was conducted by deriving and simplifying the heat balance equations for the hybrid hot storage tank, the solar collector, and the absorption system. The simulation aimed to identify the optimal wax ratio of 5% to 20% to maximize system performance. The optimal paraffin ratio was found to be 10% of the tank volume, which enabled an additional 4 hours of operation and extended the system's uptime to its maximum potential.

Corresponding Author:

Thamir Khalil Ibrahim
Department of Mechanical Engineering, College of Engineering, Tikrit University
Tikrit, Iraq
Email: thamirmathcad@tu.edu.iq

1. INTRODUCTION

Population growth increases demand for conventional energy, primarily driven by industries, transportation, and other applications worldwide [1]-[3]. Traditional compression cycle air conditioners, which consume large amounts of energy, further increase electricity consumption during the summer, especially at midday [4]. Solar energy can be used as a solution to address these issues and alleviate the strain on electricity systems that rely on traditional fossil fuels [5]. Numerous studies have been conducted on new designs incorporating solar energy to produce thermal energy for operating absorption systems, such as air-conditioning systems [6], [7]. Parabolic trough solar collectors, which drive absorption cooling systems, are more suitable for long-term air conditioning because they utilize daylight solar intensity to produce thermal energy [8]. However, this method becomes ineffective on cloudy or dusty days or at night. To address this issue, the system incorporates a thermal storage tank to extend nighttime operation of the absorption system and to store surplus heat during the day for continuous operation as long as possible [8]. A cold storage tank can also be used to store excess cooling capacity, further extending the cooling unit's operating hours at night [9], [10]. Another study examined the thermal analysis of hot and cold storage materials for a two-ton capacity lithium bromide aqueous solution absorption cycle refrigeration system. Five fluids were tested to determine the best substitutes for the hot and cold tanks. The optimal hot tank size was found to be 0.55 cubic meters, while the cold tank's optimal size was 1.5 cubic meters. Additionally, the optimal area of the concentrating solar collector is 11.7 square meters to increase operating hours. The ideal fluid identified is glycerol, which enhances operating hours and withstands high temperatures with the same tank volume and collector area [11].

Thermal storage tanks have advanced from basic water reservoirs to sophisticated thermal batteries composed of specialized materials. Yang *et al*. [12] demonstrated that well-designed storage tanks can increase absorption system run times by 8-10 hours for cooling load management. However, as noted in the meta-analysis by Mishra *et. al*. [13], conventional water-based storage is plagued by large temperature fluctuations that hinder absorption cycle efficiency. The generator unit, which requires stable heat input to maintain a constant coefficient of performance (COP), is most affected by these fluctuations. Recent developments by Lee *et al*. [14] showed that stratified storage setups with multiple temperature zones can enhance performance by 25-30%. Meanwhile, Chekifi and Boukraa [15] computational fluid dynamics study indicated that cylindrical tanks with 2:1 height-to-diameter ratios minimize thermal mixing losses. These advances pave the way for the inclusion of phase change material (PCM), which can further improve storage performance by providing isothermal conditions throughout charging and discharging operations. Phase change materials, particularly paraffin-based ones, have revolutionized thermal energy storage for cooling applications. Aiswarya *et al.* [16] comprehensive materials review identified paraffin PCM with melting points between 82-88 °C as the most suited for absorption systems, offering the best trade-off between energy density (170 kJ/kg) and thermal stability. A recent study by Mohan *et al*. [17] demonstrated that nano-enhanced paraffin composites can achieve thermal conductivities of 0.45 W/m·K, an increase of 125% compared to conventional formulations.

The current research investigates the operation of a solar-powered absorption refrigeration system with a paraffin storage tank. The proportion of paraffin to water (5–20%) is optimized for maximum energy storage, tank temperature at 85 °C, and extends the operating hours during low sun input. The COP is also compared under varying ambient conditions, justifying experimental and theoretical findings. Results confirm that thermal buffering of paraffin optimizes the availability of the system after peak sun hours. Practical uses are envisioned in high-solar regions like Tikrit, Iraq. The study confirms PCM use for effective, sustainable cooling, and proposes future development with the application of hybrid or composite PCMs.

2. METHOD

The cooling system consists of three main parts: a concentric parabolic collector, an absorption system (using ammonia and water solution), and a wax-lined (parafine PCM) in hot water storage tank. Figure 1 shows a schematic diagram of the system. Solar energy is collected by the concentric parabolic collector and used to heat the generator of the absorption cycle [18]. Excess thermal energy is stored in a hot water tank, the inner wall lined with a wax layer occupying 10% of the tank's volume. This wax melts at 85 °C, helping to maintain the tank temperature at that level. In the afternoon, hot water from the storage tank is supplied to the absorption chiller. When solar radiation decreases, the stored thermal energy maintained at or above 85 °C is used to boil ammonia vapor from the ammonia–water solution in the generator for as long as possible. In the absorption cycle, the generated ammonia vapor condenses at high pressure in the condenser. Then, it moves to the evaporator through the expansion valve, where it evaporates at low pressure. In the evaporator, the refrigerant absorbs heat directly from the conditioned space [19], meeting the cooling load. The resulting low-pressure saturated ammonia vapor is absorbed by water, forming an ammonia-rich solution in the absorbent vessel. This solution is then pumped across a heat exchanger and returned to the generator, allowing the absorption cycle to continue as long as sufficient heat is available to drive the generator [3].

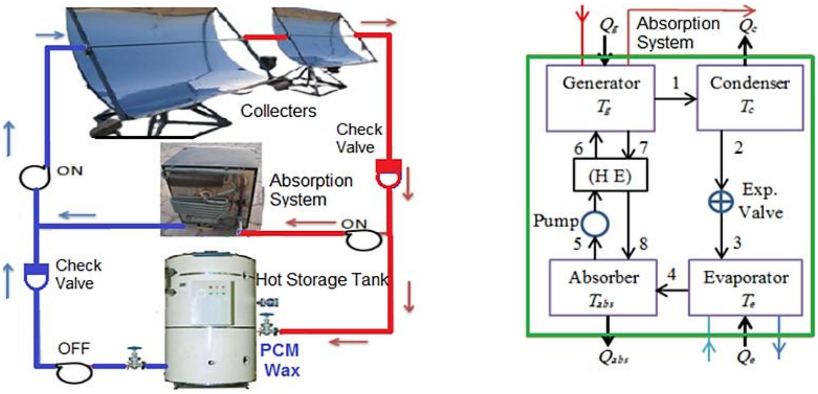

Figure 1. System diagram and schematic of the absorption cycle

The temperatures of each system component were measured hourly and recorded using a data logger. These measurements included the water temperatures entering and exiting the solar collector, the hot storage tank, the heat exchanger connected to the absorption cycle generator, the absorption vessel, the condenser, and the evaporator, as well as the ambient temperature and solar radiation intensity. Using these data, the system's operating hours were determined, and the absorption cycle performance factor was calculated for each hour of operation. Several tests were conducted during the summer months of May through August, with the most extreme conditions, such as solar radiation intensity and outdoor ambient temperatures, occurring in the first week of August (July 21, 2024). These data were used as inputs to study key system design parameters, including the hot tank size for optimal solar collector area and the paraffin ratio in the hot tank, based on the heat balance of the system.

The following assumptions were applied in simulating the components of the solar absorption cooling system and a hot storage tank:

- Fluid properties are constant, and the absorber tube flow is steady and uniform.
- Axial (longitudinal) conductive heat transfer along the tube of the absorber is neglected.
- Heat loss through connecting tubes is negligible.
- The generator and condenser operate at equal pressure; the evaporator and absorber also share equal pressure.
- The fluid exiting the generator is assumed to be saturated, the liquid leaving the condenser is saturated, and the vapor leaving the evaporator is saturated.
- The solution leaving the generator is considered at the boiling point, and the solution exiting the absorber is saturated.
- The expansion valve operates under adiabatic conditions (no heat exchange with the surroundings).
- The actual useful heat gained from the parabolic collector, Q_{Usf}, can be calculated as (1) [20].

$$Q_{Usf} = A_{Ape}F_R[H_{Rta} - \frac{A_{Rto}}{A_{Ape}}U_L(T_{Wi} - T_{Amp})] \quad (1)$$

Where A_{Rto} is the external absorber tube area, A_{Ape} is the absorber area, T_{Wi} is the inlet water temperature, the heat removal factor (F_R), U_L is the overall heat loss coefficient in the glass tube, T_{Amp} is the ambient temperature, and H_{Rtra} is the achievement of solar energy in the collector absorption tube, which can be defined as (2) [20].

$$H_{Rtra} = I_b \tau \alpha \rho \gamma \quad (2)$$

Where I_b is the solar intensity, τ is the transmittance of the absorber tube, α is the absorbance, ρ is the reflectiveness, and γ is the objection coefficient of the absorber tube [20].

An energy balance on the unstratified tank in the charging mode is given by (3). Similarly, an energy balance on the unstratified tank in the discharging mode is given by (4).

$$(M_W Cp_W)\frac{dT_{ST}}{dt_{ST}} + \dot{P_{str}} = [Q_{Usf} - G_L - (U_{ST}A_{ST})(T_{ST,Old} - T_{Amp}] \quad (3)$$

$$(M_W Cp_W)\frac{dT_{ST}}{dt_{ST}} - \dot{P_{str}} = [Q_{Usf} - G_L - (U_{ST}A_{ST})(T_{ST,Old} - T_{Amp}] \quad (4)$$

Where $\dot{P_{str}}$ is the storage power, Cp_W is the specific heat capacity of water, M_W is the mass of water, U_{ST} is the thermal overall heat transfer coefficient of the hot storage tank, G_L is the absorption cycle generator load, A_{ST} is the surface area of the storage tank, and $T_{ST,Old}$ is the old hot tank temperature before Δt_{ST} time step.

In paraffin PCM, the general equation for the power accumulated during charging and discharging is defined as (5) [21]. This represents the power variation during the charging and discharging processes.

$$\dot{P_{str}} = \frac{M_{PCM}\,[Cp_{PCM}\ x\ (T_m - T_{i-ch}) + h_f + Cp_{PCM}\ x\ (T_{f-ch} - T_m)]}{3600\ \mathrm{x}\ \Delta t_{CH}} \quad (5)$$

Where Cp_{PCM} is the specific heat capacity of paraffin PCM, M_{PCM} is the mass of paraffin PCM, h_f is the latent heat of PCM, T_m is the melting temperature of paraffin, T_{i-ch} is the temperature of paraffin at initial of charging period, Δt_{ST} is the time step, and T_{f-ch} is the temperature of paraffin at the end of the charging period. The new hot tank temperature $T_{ST,New}$ after Δt_{ST} time step in charging mod is defined as (6) [13].

$$T_{ST,New} = T_{ST,Old} + \frac{\Delta t_{ST}}{(M_w\ Cp_w)}[Q_{Usf} - \dot{P_{str}} - G_L - (U_{ST}A_{ST})(T_{ST,Old} - T_{Amp}] \quad (6)$$

The new hot tank temperature $T_{ST,New}$ after Δt_{ST} time step in the discharging mod is defined as (7) [22].

$$T_{ST,New} = T_{ST,Old} + \frac{\Delta t_{ST}}{(M_w\ Cp_w)}[Q_{Usf} + \dot{P_{str}} - G_L - (U_{ST}A_{ST})(T_{ST,Old} - T_{Amp}] \quad (7)$$

Where $T_{ST,Old}$ is the old hot storage tank temperature before time step 1 hour.

The energy balance of the generator can be described as (8) [23]. Here, $\dot{m_{1,A}}$ is the mass flow rate of the working fluid (ammonia), $\dot{m_{8,Ass}}$ is the mass flow rate of ammonia at saturation condition, $h_{1,A}$ is the ammonia enthalpy, and $h_{7,As}$ is the ammonia enthalpy at the saturation condition.

$$Q_g = \dot{m_{1,A}}h_{1,A} + \dot{m_{8,\mathrm{Ass}}}h_{8,Ass} - \dot{m_{7,As}}h_{7,As} \quad (8)$$

For the condenser, the energy balance is expressed by (9) [24].

$$Q_c = \dot{m_{1,A}}h_{1,A} - \dot{m_{2,A}}h_{2,A}) \quad (9)$$

For the expansion valve, the energy balance is expressed by (10).

$$h_{2,A} = h_{3,A} \quad (10)$$

For the evaporator, the energy balance is expressed by (11) [25].

$$Q_e = \dot{m_{4,A}}h_{4,A} - \dot{m_{3,A}}h_{3,A} \quad (11)$$

For the pump solution, the energy balance is expressed by (12) [25].

$$w_p = \dot{m_{6,As}}h_{6,As} - \dot{m_{5,As}}h_{5,As} \quad (12)$$

For the absorber, the energy balance is expressed by (13) [26].

$$Q_{abs} = \dot{m_{4,A}}h_{4,A} + \dot{m_{10,Ass}}h_{10,Ass} - \dot{m_{5,As}}h_{5,ws} \quad (13)$$

The final energy balance is obtained as (14).

$$Q_g + Q_e = Q_c + Q_{abs} \quad (14)$$

For heat exchanger, the energy balance is expressed by (15).

$$Q_e = \dot{m_{8,Ass}}(h_{8,\mathrm{Ass}} - h_{9,Ass}) = \dot{m_{7,As}}(h_{7,As} - h_{6,As}) \quad (15)$$

The COP of the absorption system is expressed by (16) [26].

$$COP = \frac{Q_e}{Q_g} \quad (16)$$

The experimental part of this study investigates the performance of an absorption cooling system by incorporating paraffin into the lining of the hot storage tank to stabilize the tank temperature at the paraffin's melting point. Paraffin, having the properties shown in Table 1, with an optimum volume to water storage tank ratio of 10%, is used as a filler to enhance thermal storage stability, based on a mathematical model that applies thermal equilibrium principles. The system consists of parabolic trough solar collectors, a hot storage tank, and the absorption system, as shown in Figure 1. The charging process of warming the hot storage tank is shown in Figure 2(a), while Figure 2(b) illustrates energy discharge from the hot storage tank.

Thermometers are installed to measure temperatures at various locations, including inside the tank, within the paraffin, on the tank wall, and across components of the absorption system such as the generator, condenser, evaporator, and absorber. A thermometer is also positioned to measure the temperature of the fluid exiting the heat exchanger between the generator and the absorber. Environmental parameters such as ambient temperature, wind velocity, and solar radiation are recorded using sensors connected to a data logger, which transmits the data to a computer for hourly logging. The cooling load of the room, which varies throughout the day depending on ambient conditions, is also calculated, representing the cooling capacity of the absorption system. This experimental data enables the hourly calculation of the absorption cycle's COP during actual operation. Additionally, the experimental study evaluates the operating time of the absorption system depending on the hot storage tank, with and without PCM paraffin, as shown in Table 1. The actual operating hours are then compared with the theoretical values derived from heat balance equations. The COP is calculated for each operating hour using experimental data and theoretical models to assess the level of agreement and identify any deviations between them.

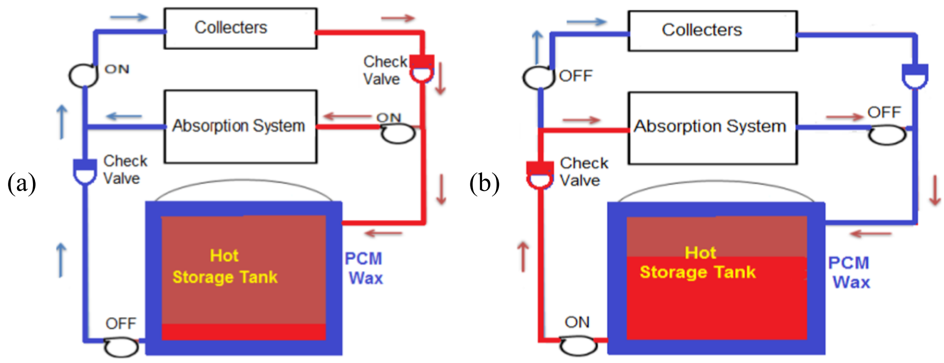

Figure 2. Schematic of the hot storage tank during (a) charging and (b) discharging modes

Table 1. Simulation results

No.	Criteria ot the most important data	Typical values
1	Melting area	82–85 °C
2	Heat storage capacity	170 kJ/kg
3	Specific heating capacity	2 kJ/(kg·K)
4	Density solid	0.88 kg/L
5	Density liquid	0.77 kg/L
6	Heat conductivity (both phases)	0.2 W/(m·K)
7	Volume expansion	12.5%
8	Flash point	< 200 °C
9	Max. operation temperature	100 °C

3. RESULTS AND DISCUSSION

Figure 3 illustrates the daily variation in dry bulb ambient temperature and solar radiation in the study area, Tikrit City, located in central Iraq, on July 21, 2024, during the summer season. Significant fluctuations in dry bulb temperature are observed from sunrise to sunset, particularly between 9:00 a.m. and 4:00 p.m., with peak temperatures occurring approximately two hours after noon. The figure also shows the hourly variation in solar radiation on the same day. Solar radiation intensity increases after sunrise, peaks around midday, and gradually declines toward sunset. The maximum solar radiation is recorded near noon, typically preceding the peak dry bulb temperature by about two hours. Solar radiation remains minimal or absent during the early morning and nighttime hours. These climatic conditions, characterized by high ambient temperatures [27], [28] and intense solar radiation, are favorable for the operation of solar-driven absorption cooling systems, which rely on thermal energy from the sun. As a result, such systems are particularly effective and well-suited for providing cooling in this region.

Figures 4 to 7 illustrate the variation of measured water temperature over time in a one-cubic-meter hot water tank and an equivalent 10-square-meter parabolic concentric collector area used for air conditioning a room with an absorption system. The room's cooling load varies hourly depending on environmental conditions throughout the day. Each figure includes two curves, one with and one without Prarafine PCM, corresponding to different PCM volume percentages ranging from 5% to 20%. Figure 3 shows that the temperature of the water containing 5% paraffin remains lower than that of the water without paraffin during the daytime, especially when solar radiation is at its peak. This behaviour occurs because the paraffin absorbs heat until it reaches its melting point, which remains constant while storing energy as latent heat. The paraffin continues to absorb heat at a constant temperature of 85 °C for approximately two hours, without disrupting the operating conditions of the absorption system. Once fully melted, the PCM remains liquid and stores the excess heat as sensible heat. After sunset, the temperature drops to saturation and stays there for an additional three hours, enabling the absorption system to continue operating under suitable thermal conditions.

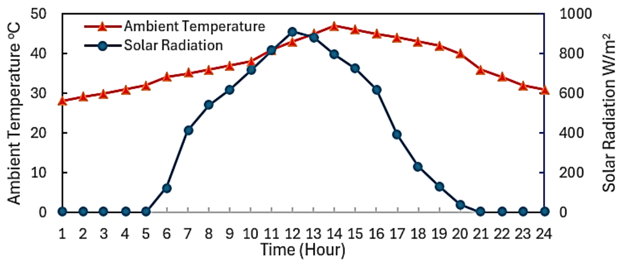

Figure 3. The variation in temperature and solar radiation intensity throughout the day

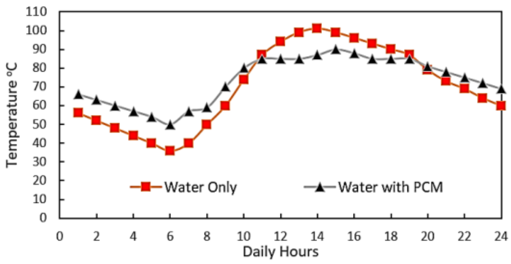

Figure 4. The temperature variation of water with and without 5% PCM throughout the day

Figure 5 shows that the temperature of the water containing 10% paraffin remains lower than that of the water without paraffin during the daytime. The PCM paraffin absorbs heat until it reaches its melting point, which remains constant while storing energy as latent heat. This operation does not interfere with the working conditions of the absorption system. Once the paraffin completely melts, the PCM remains solid if there isn't enough heat to continue with further phase change. It stores excess heat as sensible heat when solar intensity decreases before sunset. At sunset, the temperature reaches a saturation point and remains there for a few hours, allowing the absorption system to operate under optimal thermal conditions. Figure 6 shows that the temperature of the water containing 15% paraffin remains lower than that of the water without paraffin during the day. The PCM paraffin absorbs heat until it reaches its melting point of 85 °C. At this point, the temperature stabilizes as the paraffin stores energy as latent heat. This heat absorption process does not affect the operating conditions of the absorption system. Once the paraffin is fully melted, the PCM remains solid when the available heat isn't enough to cause further phase change. It stores extra heat as sensible heat as solar irradiance diminishes approaching sunset. The temperature stays steady at approximately 85 °C for nearly three hours, which is enough to keep the absorption system running during this period.

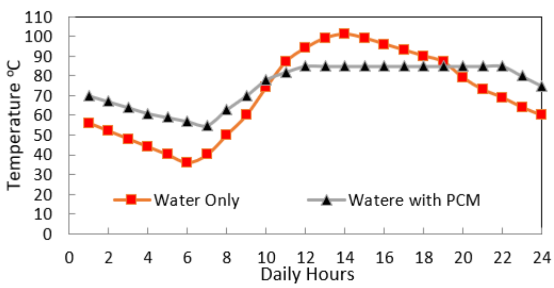

Figure 5. The temperature variation of the hot storage tank water with and without 10% PCM throughout the day

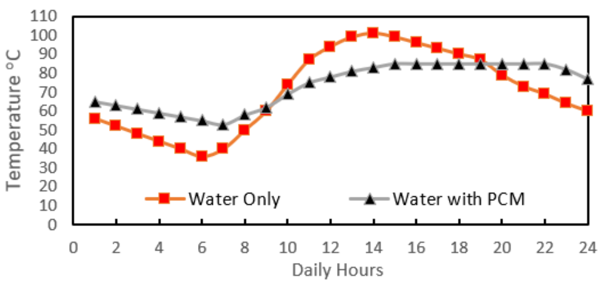

Figure 6. The temperature variation of water with and without 15% PCM throughout the day

Figure 7 shows that the water containing 20% paraffin remains lower than the water without paraffin during the day, as the increased paraffin content requires more heat to raise its temperature. The PCM paraffin absorbs heat until its melting point of 85°C. Due to the greater amount of paraffin, additional heat and time are needed for the temperature to stabilize as the paraffin stores energy in the form of latent heat. This heat absorption process affects the operation of the absorption system during daylight hours. Since the available heat is insufficient to complete the phase change, the PCM remains solid and stores excess heat as sensible heat as solar intensity decreases toward sunset. The temperature stabilizes at around 85 °C for less than three hours, which is insufficient for sustained system operation during that period. Additionally, the system may not reach the desired temperature during the early daylight hours. This behaviour enhances the performance of the solar collectors by extending their effective operating range and preventing the water from reaching its boiling point around midday.

Figures 8–11 illustrate the relationship between the number of operational hours at a water temperature (83–85 °C), suitable for absorption cycle operation, and the temperature in a 1-cubic-meter hot water tank. The energy balance was calculated using a real cooling load that varies with ambient conditions and a 10-square-meter parabolic concentric collector supplying the absorption system. These figures include statistical bars representing the system's operating temperature, both with and without PCM, for PCM volume fractions ranging from 5% to 20%. Figure 8 shows that during the early morning hours, the hot storage tank maintains water at 85 °C for a shorter duration in the tank containing 5% paraffin than in the tank without paraffin. The onset of the optimal operating temperature is delayed by approximately one hour; however, this period extends by several additional hours in the afternoon. This behavior is due to paraffin, which acts as a PCM. The PCM absorbs heat until it reaches its melting point, storing energy as latent heat while maintaining a constant temperature of 85 °C. It continues to absorb heat at this temperature for some time, then remains in a liquid state and stores additional energy as sensible heat, without disrupting the operation of the absorption cooling system. As solar radiation decreases and the temperature drops in the afternoon, the PCM starts to solidify at its melting point. This phase transition helps sustain the system's operation at the optimal temperature of 85 °C for approximately two additional hours.

Figure 9 shows that during the pre-afternoon period, the water temperature in the heated storage tank remains around 85 °C for more hours in the tank containing 10% paraffin compared to the tank with water only. This is due to the properties of paraffin as a PCM. The PCM is heated until it melts at its melting point, where the energy is stored as latent heat, maintaining a constant temperature of 85 °C. When fully melted and when solar radiation decreases, causing the water temperature to fall in the afternoon, the PCM begins to solidify at its melting point. This phase transition releases the trapped latent heat, helping to keep the hot storage tank at the required 85 °C for about four hours longer.

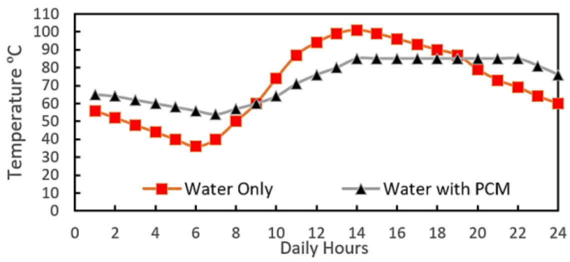

Figure 7. The temperature variation of water with and without 20% PCM throughout the day

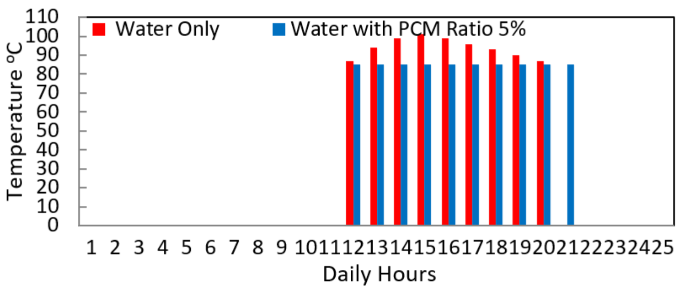

Figure 8. The water temperature variations with and without 5% PCM and the operating hours of the absorption system throughout the day

Figure 10 shows that during the pre-afternoon hours, the storage tank with 15% paraffin content maintains a water temperature of 85 °C and does not exceed it. Unlike water-only tanks, the PCM absorbs excess heat from the solar collectors during its phase transition from solid to liquid. The PCM absorbs heat until it reaches its melting point, storing the energy as latent heat while maintaining a constant temperature of 85 °C. Once fully melted, and as solar irradiance decreases in the afternoon, the PCM begins to solidify at its melting point. This phase transition releases the stored latent heat, allowing the heated storage tank to maintain the optimal temperature of 85 °C for approximately three additional hours. However, increasing the PCM content above 15% did not significantly improve heat storage, indicating that the additional paraffin had little effect on the total amount of heat stored. Figure 11 shows that during the pre-noon hours, the heated storage tank maintains a water temperature of 85 °C for a shorter period in the tank containing 20% paraffin, compared to the tank containing 15% paraffin and the tank without paraffin. This is because the additional paraffin requires more heat to heat it to its melting temperature. The PCM continues to absorb heat until it reaches its melting point, storing the energy as latent heat while maintaining a constant temperature of 85 °C. However, as solar irradiance decreases, the PCM begins to solidify at its melting point, allowing the system to maintain the optimal temperature of 85 °C for the same period. However, increasing the PCM content above 20% did not improve heat storage, indicating that the additional paraffin did not affect the total amount of heat stored.

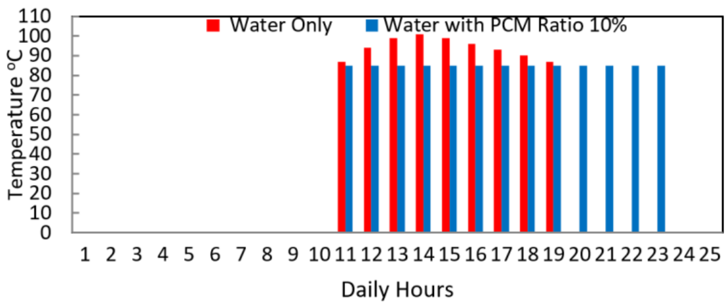

Figure 9. Daytime operating time of the absorption system and water temperature changes with and without 10% PCM

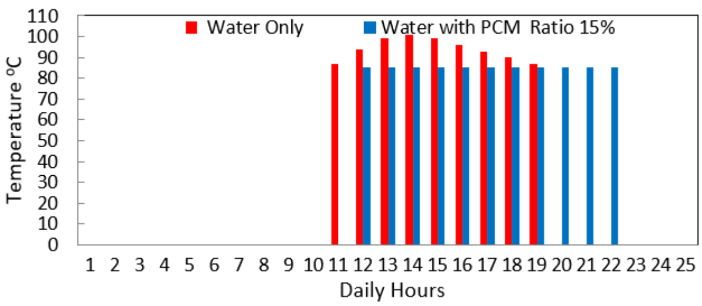

Figure 10. The operating hours of the absorption system throughout the day and the water temperature variations with and without 15% PCM

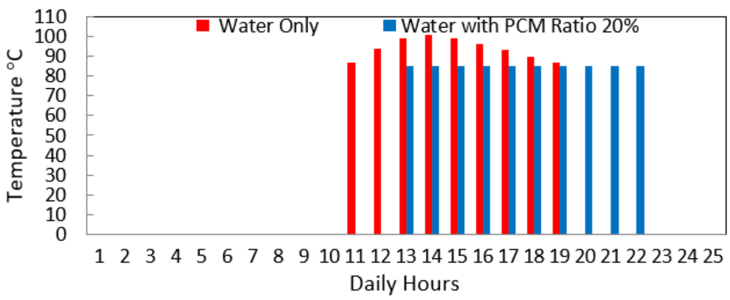

Figure 11. The operating hours of the absorption system throughout the day and the water temperature variations with and without 20% PCM

Figure 12 shows the operating hours of a hot tank containing different PCM concentrations. Typically, the water tank not only maintains a temperature of 85 °C, but also exceeds it and may even reach the boiling point of water. Meanwhile, a tank with 5% PCM maintains a temperature below the boiling point of water. The most extended system runtime is observed at 10% PCM. Although the onset of optimal operating temperature is delayed by about an hour before noon, the system continues to operate for several additional hours after sunset. After the PCM concentration exceeds 10%, 15 %, and 20%, operating hours decrease; this decrease is attributed to the increased heat required to melt the additional paraffin, which exceeds the current design capacity of the collector. While increasing the collector area may address this limitation, it results in a trade-off between extended operating hours, collector size, and PCM ratio content. The goal is to determine an optimal design that meets the required cooling capacity based on the room's cooling load. The phase change material absorbs heat until it reaches its melting point, storing it as latent heat while maintaining a constant temperature of 85 °C. This process prevents the hot tank from overheating during the afternoon when solar radiation intensity increases. Once the PCM is completely melted, the energy is stored as sensible heat without affecting the absorption cooling system's operation, as long as it does not exceed the boiling point of water. As solar radiation decreases and ambient temperatures drop in the afternoon, the PCM begins to solidify at its melting point. During this phase transition, the stored latent heat is released, helping to maintain the system's optimal operating temperature of 85 °C. This extends the cooling system's operation for several hours into the evening, even after sunset.

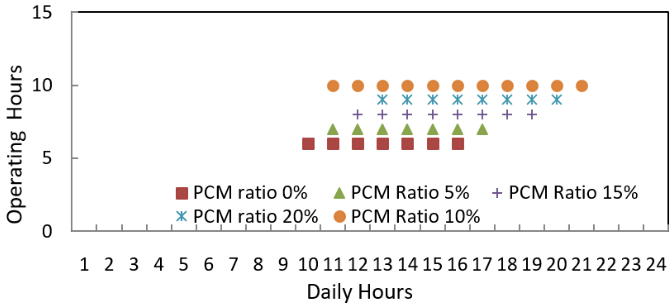

Figure 12. The variation in operating hours for different PCM ratio

Figure 13 illustrates the variation in the COP over a day based on experimental and theoretical results. The hourly coefficient of performance is calculated from experimental measurements taken when the water temperature in the hot tank reaches 85 °C, which is the operating temperature needed for the absorption system. The system uses a 1-cubic-meter hot tank, a 10-square-meter solar collector area, and contains 10% paraffin. The number of operating hours is recorded, and after measuring the temperatures of the absorption system components, the coefficient of performance is determined using (8) to (16). The theoretical coefficient of performance is calculated under the same design and environmental conditions but based on a thermal balance performed using (1) to (16). Generally, both curves begin at relatively high values before noon and then decline, reaching their lowest point around 2:00 p.m., when ambient temperatures peak. The COP values then rise again as the afternoon progresses. This trend is attributed to the absorption system using ambient air to cool its condenser. As the ambient temperature increases, the temperature difference between the condenser and the surrounding environment decreases, reducing the system's heat rejection capacity and consequently lowering the COP. Conversely, heat rejection improves as the temperature difference increases later in the day, resulting in a higher COP. The discrepancy between the theoretical and experimental results is slight (less than 5%), indicating a high degree of accuracy in the thermal balance. This subtle difference is expected and can be attributed to the precision of the measurement instruments and the assumptions made in the theoretical thermal analysis.

Figure 14 displays the daily variation of the actual COP of the absorption refrigeration cycle. The system begins at 10:00 a.m., operating with only the hot water tank, and at 11:00 a.m., it operates with a tank containing 10% more paraffin. This delay is due to the additional time needed to heat the extra paraffin in the tank. Although solar radiation intensifies toward midday, the functional COP decreases as the day advances. This decline is caused by the rising ambient air temperature, which impacts the heat dissipation process in the absorption system's condenser. The system activates when the tank temperature reaches 85 °C, sufficient to initiate the absorption refrigeration cycle generator. While the generator's temperature remains relatively stable, the actual COP varies with the paraffin and storage tank conditions. Changes in ambient temperature throughout the day, especially in the afternoon, influence the condenser's ability to release heat into the environment. The inclusion of paraffin enhances the system's thermal storage efficiency due to the properties of the PCM. The latent heat stored in the paraffin helps maintain the tank's temperature near the phase change point, allowing the system to operate for extended periods. This also expands the effective area of the solar collector, which heats the hot water tank without reaching a boiling point. Consequently, the system can operate until around 10:00 PM with the paraffin-enriched tank, compared to about 6:00 PM with the water tank. Using paraffin markedly increases the heat storage capacity, enabling more consistent and extended operation of the absorption refrigeration cycle with an improved coefficient of performance.

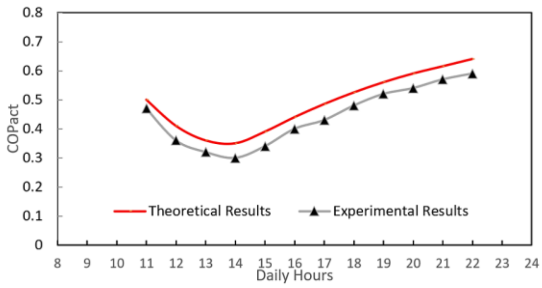

Figure 13. Comparison between experimental and theoretical COP

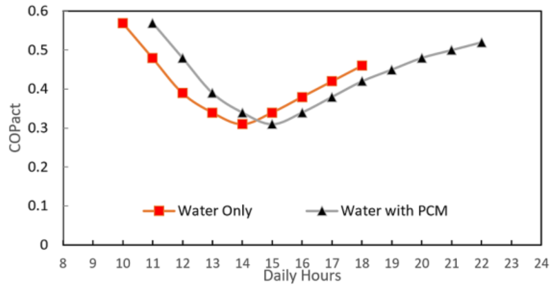

Figure 14. The variation in COP throughout the day depends on the presence of a water storage tank, both without and with 10% PCM

4. CONCLUSION

This study confirmed that adding a paraffin PCM (10% of tank volume) to a solar absorption cooling system significantly improved thermal efficiency. The PCM maintained a steady 85 °C tank temperature, preventing overheating during intense radiation and extending daily operation by 4 hours (total 11 hours) compared to water-only setups. Latent heat storage acted as a buffer by storing excess solar energy during the day and releasing it after sunset, stabilizing the system. Experimental results validated the thermal model, showing less than 5% variation in COP values and peak efficiency during cooler morning and evening times. The analysis identified 10% PCM as optimal; lower percentages (5%) offered minimal improvements, while higher percentages (15-20%) required more heat input. These findings support using PCM in high-solar-latitude regions like Iraq, where it extends operation without larger collectors. The research provides practical recommendations for deploying PCM-assisted cooling systems powered by renewable energy. Future studies could explore hybrid PCM mixtures or incorporate cold storage to enhance system performance further.

ACKNOWLEDGMENTS

We sincerely thank the College of Engineering at Tikrit University for its comprehensive support in completing this research.

FUNDING INFORMATION

There is no funding for this study.

AUTHOR CONTRIBUTIONS STATEMENT

This journal uses the Contributor Roles Taxonomy (CRediT) to recognize individual author contributions, reduce authorship disputes, and facilitate collaboration.

Name of Author	C	M	So	Va	Fo	I	R	D	O	E	Vi	Su	P	Fu
Maki Haj Zaidan	✓	✓	✓	✓	✓	✓		✓	✓	✓			✓	
Thamir Khalil Ibrahim		✓		✓	✓	✓		✓	✓	✓	✓	✓		✓
Hussam S. Dheyab	✓		✓				✓			✓	✓		✓	

C : **C**onceptualization
M : **M**ethodology
So : **So**ftware
Va : **Va**lidation
Fo : **Fo**rmal analysis
I : **I**nvestigation
R : **R**esources
D : **D**ata Curation
O : Writing - **O**riginal Draft
E : Writing - Review & **E**diting
Vi : **Vi**sualization
Su : **Su**pervision
P : **P**roject administration
Fu : **Fu**nding acquisition

CONFLICT OF INTEREST STATEMENT

The authors state no conflict of interest.

DATA AVAILABILITY

The data that support the findings of this study are available on request from the corresponding author, [TKI]. The data, which contain information that could compromise the privacy of research participants, are not publicly available due to certain restrictions.

REFERENCES

[1] M. A. Qasim and T. H. Atyia, "Design and implementation of VSI for solar water pump control," *Tikrit Journal of Engineering Sciences*, vol. 31, no. 1, pp. 193–210, 2024, doi: 10.25130/tjes.31.1.17.

[2] J. Fernandes, C. Pimenta, R. Mateus, S. M. Silva, and L. Bragança, "Contribution of Portuguese vernacular building strategies to indoor thermal comfort and occupants' perception," *Buildings*, vol. 5, no. 4, pp. 1242–1264, 2015, doi: 10.3390/buildings5041242.

[3] M. Fan, H. Liang, S. You, H. Zhang, B. Yin, and X. Wu, "Applicability analysis of the solar heating system with parabolic trough solar collectors in different regions of China," *Applied Energy*, vol. 221, pp. 100–111, Jul. 2018, doi: 10.1016/j.apenergy.2018.03.137.

[4] A. A. Gitan and A. H. Mohammed, "Assessment of perforated double-pass solar air heater using parametric interaction analysis for performance enhancement in solar thermal systems," *Tikrit Journal of Engineering Sciences*, vol. 31, no. 3, pp. 177–191, 2024, doi: 10.25130/tjes.31.3.17.

[5] G. Al-Doori, O. H. Al Naamani, and G. T. Chala, "Effect of phasechange material heated by solar energy on the flow assurance of heavy crude oil," *Tikrit Journal of Engineering Sciences*, vol. 32, no. 2, 2025, doi: 10.25130/tjes.32.2.18.

[6] I. S. Farhan, A. A. Mohammed, and M. S. M. Al-Jethelah, "The effect of uneven metal foam distribution on solar compound parabolic trough collector receiver thermal performance," *Tikrit Journal of Engineering Sciences*, vol. 31, no. 1, pp. 291–305, 2024, doi: 10.25130/tjes.31.1.24.

[7] C. Cornaro, G. Basciano, V. A. Puggioni, and M. Pierro, "Energy saving assessment of semi-transparent photovoltaic modules integrated into NZEB," *Buildings*, vol. 7, no. 1, 2017, doi: 10.3390/buildings7010009.

[8] K. M. A. Kabir, K. C. A. Alam, M. M. A. Sarker, R. A. Rouf, and B. B. Saha, "Effect of mass recovery on the performance of solar adsorption cooling system," *Energy Procedia*, vol. 79, pp. 67–72, 2015, doi: 10.1016/j.egypro.2015.11.479.

[9] M. H. Zaidan, H. J. Khalaf, and B. A. Ahmed, "Thermal analysis of a solar absorption cooling system with hot and cold storage tanks," *Journal of Advanced Research in Fluid Mechanics and Thermal Sciences*, vol. 50, no. 1, pp. 67–80, 2018.

[10 M. N. Al–maliki, M. Soldan, H. A. Issa, L. M. Abdali, B. A. Yakimovich, and H. Kobeticova, "The performance and advanced cooling techniques for photovoltaic solar panels," *MM Science Journal*, vol. 2024, pp. 7782–7787, 2024, doi: 10.17973/MMSJ.2024_11_2024055.

[11] M. H. Zaidan and M. K. Daham, "Thermal analysis for the materials of the hot and cold storage tanks for a cooling system operating by absorption cycle," in *AIP Conference Proceedings*, 2020, vol. 2213, doi: 10.1063/5.0000458.

[12] X. Yang, Y. Li, Y. Ma, J. Cui, and J. Xie, "Optimization of thermal storage performance of cascaded multi-PCMs and carbon foam energy storage system based on GPR-PSO algorithm," *Journal of Energy Storage*, vol. 83, p. 110626, Apr. 2024, doi: 10.1016/j.est.2024.110626.

[13] A. K. Mishra *et al.*, "Dynamic PCM strategies with nano-enhanced composites for optimal thermal energy storage and management," *Chemical Engineering Journal Advances*, vol. 23, p. 100789, Aug. 2025, doi: 10.1016/j.ceja.2025.100789.

[14] S. Lee *et al.*, "Optimization and performance analysis of PCM heat sink with flat heat pipes under extreme thermal loads," *Applied Thermal Engineering*, vol. 277, p. 127032, Oct. 2025, doi: 10.1016/j.applthermaleng.2025.127032.

[15] T. Chekifi and M. Boukraa, "CFD applications for sensible heat storage: a comprehensive review of numerical studies," *Journal of Energy Storage*, vol. 68, 2023, doi: 10.1016/j.est.2023.107893.

[16] V. Aiswarya, S. Das, A. James, S. K. Saha, and B. B. Saha, "An experimental investigation on the solar thermal energy storage potential of form stabilized paraffin microcapsules," *Journal of Environmental Chemical Engineering*, vol. 13, no. 3, p. 116825, Jun. 2025, doi: 10.1016/j.jece.2025.116825.

[17] M. Mohan *et al.*, "Optimization of synthesis parameters for copper oxide-enhanced phase change material: balancing thermal conductivity and latent heat trade-off," *Thermal Science and Engineering Progress*, vol. 59, p. 103334, Mar. 2025, doi: 10.1016/j.tsep.2025.103334.

[18] H. F. Saleh, M. A. Eleiwi, and N. D. Mokhlif, "Improving the performance of a home solar water heater system using porous materials and reflectors," *Tikrit Journal of Engineering Sciences*, vol. 31, no. 2, pp. 244–254, 2024, doi: 10.25130/tjes.31.2.23.

[19] R. Ben Iffa, N. Bouaziz, and L. Kairouani, "Optimization of absorption refrigeration systems by design of experiments method," *Energy Procedia*, vol. 139, pp. 280–287, Dec. 2017, doi: 10.1016/j.egypro.2017.11.209.

[20] A. Mahmoudi, P. Esfanjani, S. Rashidi, M. S. Valipour, and W.-M. Yan, "Potentials of parabolic dish collectors in sustainable decentralized thermal applications: a comprehensive review," *Applied Thermal Engineering*, vol. 275, p. 126911, Sep. 2025, doi: 10.1016/j.applthermaleng.2025.126911.

[21] A. K. Raj, M. Srinivas, and S. Jayaraj, "A cost-effective method to improve the performance of solar air heaters using discrete macro-encapsulated PCM capsules for drying applications," *Applied Thermal Engineering*, vol. 146, pp. 910–920, Jan. 2019, doi: 10.1016/j.applthermaleng.2018.10.055.

[22] M. Yang, M. A. Moghimi, R. Loillier, C. N. Markides, and M. Kadivar, "Design of a latent heat thermal energy storage system under simultaneous charging and discharging for solar domestic hot water applications," *Applied Energy*, vol. 336, p. 120848, Apr. 2023, doi: 10.1016/j.apenergy.2023.120848.

[23] Y. Du *et al.*, "Theoretical model and application potential of hybrid passive cooling for power yield improvement of thermoelectric generators," *Energy*, vol. 327, p. 136367, Jul. 2025, doi: 10.1016/j.energy.2025.136367.

[24] Y. Li, T. Liu, and J. Sui, "Thermodynamic analysis and optimization of a distributed combined cooling and power system based on solar thermochemistry and thermal storage," *Applied Thermal Engineering*, vol. 269, p. 125996, Jun. 2025, doi: 10.1016/j.applthermaleng.2025.125996.

[25] Y. Zhi, S. Liu, B. Yang, and X. Yu, "Analysis of the thermal performance of parabolic solar dish collector using MCRT-FVM coupled optical-thermal model," *Energy*, vol. 322, p. 135579, May 2025, doi: 10.1016/j.energy.2025.135579.

[26] A. Rajan and K. S. Reddy, "Integrated optical-thermal model to predict the performance of a solar parabolic dish collector for process heating applications," *Energy*, vol. 321, p. 135176, Apr. 2025, doi: 10.1016/j.energy.2025.135176.
[27] M. H. Zaidan, F. M. Abed, and A. S. Farhad, "The effect of dry and wet bulb temperature variation on the performance of the indirect evaporative cooler," *Tikrit Journal of Engineering Sciences*, vol. 26, no. 4, pp. 8–15, 2019, doi: 10.25130/tjes.26.4.02.
[28] M. H. Zaidan, A. A. R. Alkumait, A. Q. Abdullah, and T. K. Ibrahim, "The enhancement of performance coefficient by spraying water on the condenser of the compression cooling cycle," *Journal of Advanced Research in Fluid Mechanics and Thermal Sciences*, vol. 120, no. 1, pp. 140–150, Aug. 2024, doi: 10.37934/arfmts.120.1.140150.

BIOGRAPHIES OF AUTHORS

Maki Haj Zaidan is working as a lecturer in the Mechanical Engineering Department, College of Engineering. He received his B.Sc. and B.Eng. from Baghdad University, Iraq. He completed his M.S. at the University of Tikrit, Iraq, and his Ph.D. at the University of Technology, UK. He has conducted research, provided industrial consultancy, and published over fifty papers in his area of expertise. More than 42 graduate students have completed their research under his supervision. He can be contacted at email: makihajzaidan@tu.edu.iq.

Thamir Khalil Ibrahim is a lecturer in the Mechanical Engineering Department, University of Tikrit. His research interest focused on the thermo-fluid area, such as power plants, heat transfer, cooling systems, thermoelectric generation, renewable energies, internal combustion engines, and optimizations for these systems. He can be contacted at email: thamirmathcad@tu.edu.iq.

Hussam S. Dheyab is a lecturer in the Mechanical Engineering Department, University of Tikrit. His research interests are applications of renewable energy, applications of solar energy with energy storage systems, and treating environmental pollution using clean energy. He can be contacted at email: hussam.sami@tu.edu.iq.